Full Paper

Anodic Stripping Voltammetry: An AFM Study of Some Problems and Limitations

*Michael E. Hyde, Craig E. Banks, Richard G. Compton**

Physical and Theoretical Chemistry Laboratory, University of Oxford, South Parks Road, Oxford, OX1 3QZ, UK
*e-mail: richard.compton@chemistry.ox.ac.uk

Received: April 23, 2003
Final version: May 12, 2003

Abstract
The use of anodic stripping voltammetry for quantitative analytical measurements using solid electrodes is addressed in the light of generic limitations arising from i) electrode heterogeneity, ii) electrode morphology, iii) inhibited electrodeposition, and iv) incomplete stripping of deposited metal in the anodic sweep. It is shown, using direct imaging of electrode surfaces via AFM and optical microscopy, that each of the preceding factors may produce significant deviations from ideal electrode behavior. The use of atomic force microscopy to fully characterize any developed ASV procedures is strongly recommended. To ensure reproducible and accurate stripping voltammetry, steps should be taken to minimize the effects discussed.

Keywords: Anodic stripping voltammetry, Atomic force microscopy, Electrodeposition, Nucleation

1. Introduction

Analytical chemists can see many attractions in electrochemical stripping methods including the recognition that over 40 chemical elements, not to mention a range of organic substrates, are appropriate target analytes, competitively low detection limits reaching ca. 10^{-10} mol dm^{-3} or below in favorable cases, good accuracy and reproducibility, ease of computerization and automation of analytical procedures, and relatively simple and low cost instrumentation. Nevertheless, despite extensive work with 'model systems' it is a fair observation that major 'real world' analytical usage of voltammetric methodology has yet to realize its full potential.

The limitations arise partly because of first the fact that in many target systems encountered outside of the research laboratory, the inevitable presence of surface active materials/impurities, such as proteins, surfactants, etc., can lead to significant interference and electrode passivation problems. Second, it is now seen as at least highly desirable and probably essential to employ solid electrodes rather than the mercury ubiquitously employed in pioneering work [1–3], as a result of increasingly stringent environmental legislation in Europe and Japan [4–8]. The use of such electrodes raises issues of reproducibility and of the validity of absolute calibrations.

In the present paper we seek to highlight four possible areas in which the anodic stripping voltammetry (ASV) experiment is vulnerable to mis-quantification. Using observations made on both glassy carbon (GC) and boron-doped diamond (BDD) electrodes as substrates for ASV, first we show that the surface of some solid electrodes can be macroscopically heterogeneous. Second we report that the local morphology at a surface may control its behavior towards electrodeposition. Third the effect of surface active species on nucleation and growth of the metal under deposition conditions is examined. Finally, and perhaps most significantly, we show that incomplete stripping can occur in the detection part of the experiment. The need for surface sensitive studies and allied voltammetry to probe the fundamental aspects of metal deposition is stressed as highly desirable if reliable ASV-based analytical methods are to be developed.

2. Experimental

2.1. Reagents

All reagents were of analytical grade, used without further purification. The reagents used were: silver nitrate (Sigma, 99% +), lead nitrate (AnalaR, 99.5% +), nitric acid (Aldrich, 70%, AR grade), cadmium nitrate (Aldrich), acetate buffer (Aldrich) pH 4.8 and Triton X-100 (Aldrich). All subsequent solutions were prepared using water with a resistivity of not less than 18 MΩ cm (Vivendi water systems, UK).

2.2. Instrumentation

A three electrode arrangement was used in an electrochemical cell with a boron-doped diamond (BBD) film, or glassy carbon rod (2 mm diameter) serving as the working electrode. The BDD film used (having dimensions $5 \times 5 \times 0.535$ mm and resistance approximately 0.4 Ω) was grown

  DOI: 10.1002/elan.200302863

on graphite by chemical vapor deposition and supplied by Element 6 (formerly DeBeers) Industrial Diamond Division (Ascot, U.K.). The electrode was pressed into a PTFE mounting, with an electrical connection made through the mount to a metal stub using silver-loaded epoxy resin (RS). Before each measurement (unless otherwise stated), all electrodes were cleaned using 5μm alumina polishing compound, then thoroughly rinsed to remove any surface residue.

A standard three-electrode configuration was used, controlled by a μAutolab type II potentiostat (Eco Chemie, Utrecht, the Netherlands). Ex situ deposition was performed in a cell having a volume of approximately 25 cm^3, while a Digital Instruments fluid cell (with an approximate volume of 0.5 cm^3) was used for all in situ deposition. A more detailed description of the use of the fluid cell is given elsewhere [9]

A silver wire was used as the reference electrode for all experiments involving silver nitrate. The potential of the silver wire was measured vs. SCE over a range of $AgNO_3$ concentrations between 250 μM and 5 mM, and showed a potential response of ca 61 mV per decade at 25 °C. All potentials for the $AgNO_3$ systems reported in this paper are therefore measured vs. the equilibrium potential for Ag/Ag^+ in the particular concentration of Ag^+ employed. In all other cases, a saturated calomel reference (Radiometer, Copenhagen, Denmark) was used. A bright platinum wire was used as the counter electrode throughout.

The ultrasonic horn used in this work was a Model CV 26 (Sonics and Materials Inc. USA) with an operating frequency of 20 kHz fitted with a 2 mm diameter titanium alloy microtip (Jencons, Leyton Buzzard, UK). The intensity of the ultrasound was determined calorimetrically [10, 11] and was used at powers of 155 W cm^{-2}. The working electrode was placed in a face on arrangement [12] to the ultrasonic horn with a horn tip to working electrode distance of 14 mm.

All optical images were obtained using a Digital Instruments OMV-PAR microscope based on a Sony XC-999P CCD camera, having a maximum resolution of 752×582 pixels over an area of 540×400 μm, connected to a Hauppauge video capture card. All images used in the following sections were of a size as large as the camera's maximum, in order to minimize any loss of resolution.

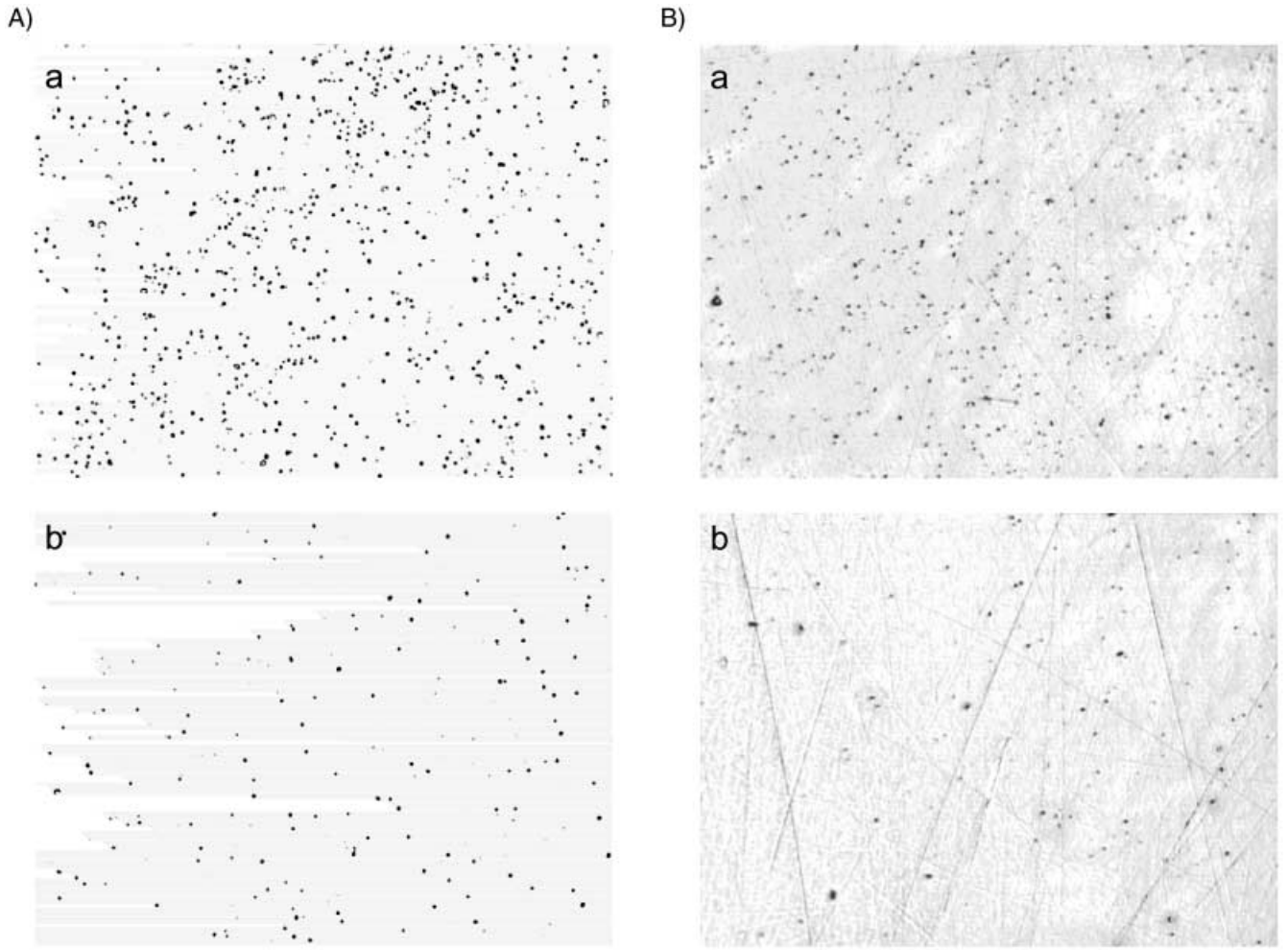

Fig. 1. Microscopic images of lead deposited from a solution containing 5 mM $PbNO_3$/0.1 M HNO_3 on A) BDD and B) GC, showing in each case a) the area of highest deposition density and b) area of lowest deposition density (see text). Deposition conditions: −0.48 V (vs. SCE) for 60 s. Images show a total area of 540×400 μm.

The AFM used was a Digital Instruments Multimode SPM, operating in ex situ contact mode. A model 'J' scanner was used, having a lateral range of 125×125 μm and a vertical range of 5 μm. Standard silicon nitride probes (type NP), having a force constant of approximately 0.58 Nm^{-1} were used.

3. Results and Discussion

3.1. Electrode Heterogeinity

In order to investigate the long range spatial homogeneity of the BDD and GC electrodes as substrates for the ASV experiment, lead was deposited from a solution containing 5 mM lead nitrate and 0.1 M nitric acid.

We find that the mean deposit density may vary widely over distances of hundreds of microns or millimeters. Deposition of lead at -0.48 V (vs. SCE) for 60 s from the solution above on both BDD and GC shows such an effect: After deposition, the entire electrode was examined optically and Figures 1A and 1B show images (of size 540×400 μm) having the highest and lowest density for each electrode material. Although the nuclei appear to have roughly the same size distribution (of the order of 2 – 4 μm in diameter), there is a significant variation in nucleus density in each case, with approximate mean nucleus densities of 2.5×10^5 and 8.5×10^4 cm^{-2} respectively in the case of both BDD and GC.

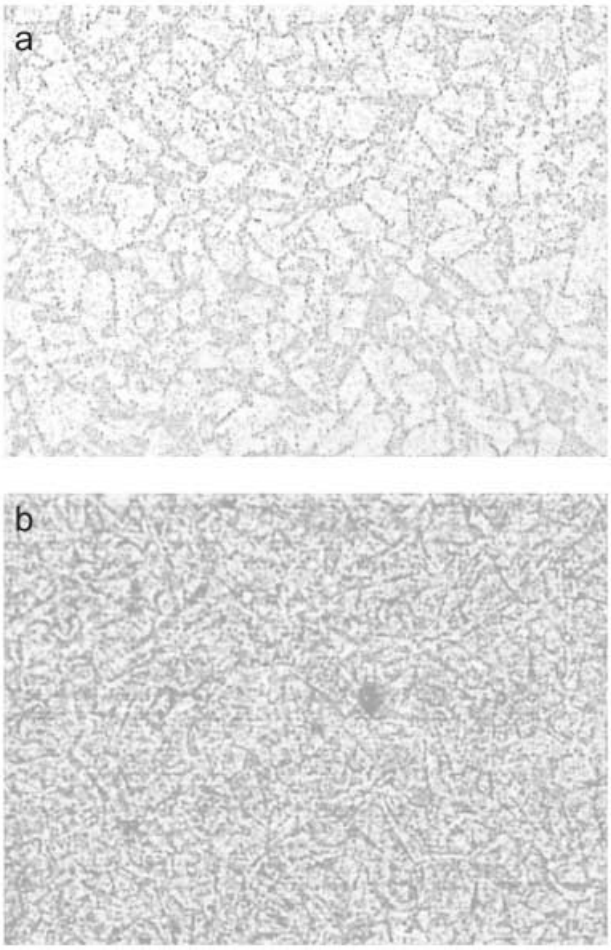

Fig. 2. Microscopic images of a) silver deposited from a solution containing 5 mM $AgNO_3$/0.1 M HNO_3 at -0.3 V (vs. Ag) for 5 s and b) lead deposited from a solution containing 5 mM $PbNO_3$/0.1 M HNO_3 at -0.6 V (vs SCE) for 5 s on BDD. Image area: 540×400 μm.

3.2. Electrode Morphology Effects

As well as variations in the long range deposition densities, local features of the electrode morphology may have a significant effect on the manner in which material is deposited in ASV experiments. A particular example of this on BDD is the effect of the polycrystalline nature of the surface of the film: on the bare electrode, regions of higher and lower reflectivity are visible under an optical microscope, corresponding to different crystal faces. This effect is clearly visible in Figure 7a, which shows a BDD surface, freshly cleaned by polishing with 1 μm alumina.

These crystal faces, as well as their differing optical properties, very probably have differing conductivities [9]. An optical image of the deposition of silver from a solution containing 5 mM $AgNO_3$ and 0.1 M HNO_3 on BDD at -0.3 V (vs. Ag) after 5 s is shown in Figure 2a. A similar patterning of the deposit on BDD may be observed with lead: deposition at -0.6 V (vs. SCE) for 5 s from the 5 mM solution produced the image in Figure 2b. Clearly there is considerable inhomogeneity in the deposit density on a scale of tens of microns, and the shape of the crystal faces can easily be seen, particularly in the case of silver. This result is consistent with different crystal faces having different conductivities; however, it should be noted that relatively large deposition potentials (-0.6 V vs. SCE and above in the case of lead) are required to achieve this kind of patterning effect. Lower deposition potentials (below approximately -0.5 V), such as those used to generate Figure 1, show no such patterning; the distribution of nuclei is essentially random.

In contrast, as might be expected from its amorphous nature, GC shows no such short range effect when a sufficiently large deposition potential is applied [13]. When silver is deposited on GC from a 5 mM solution at -0.3 V (vs. Ag) for 5 s, the distribution of nuclei appears entirely random, indicating no spatial inhomogeneity over a range of 80 μm. However, at lower deposition overpotentials, we find that GC shows morphology effects of its own, a particular example being the scratches on manually polished GC. As the backgrounds of Figures 1B and 3 show, after polishing to a mirror finish using 1 μm diamond polishing compound, the GC surface is covered in a network of scratches of various sizes. The largest of these tend to act as favorable nucleation sites, particularly at low deposition overpotentials. Illustrated in Figure 3 are examples of this effect using both 5 mM silver (at a deposition potential of

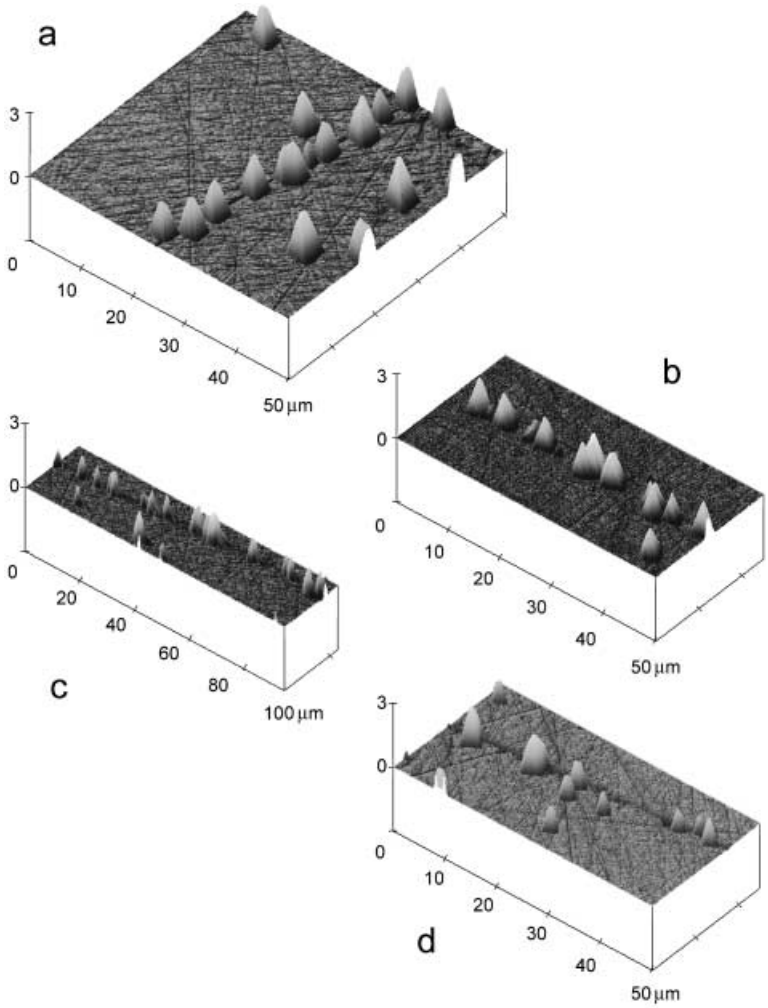

Fig. 3. AFM images of preferential metal deposition along scratch lines on GC. a–c) deposition from a 5 mM $AgNO_3$/0.1 M HNO_3 solution at −0.05 V (vs. Ag) for 120 s; d) 5 mM $PbNO_3$/0.1 M HNO_3 solution at −0.5 V (vs. SCE) for 120 s.

−0.05 V vs. Ag) and 5 mM lead (at −0.5 V vs. SCE). Although nucleation does occur at other points on the electrode, clearly there is a strong preference for appearance along certain scratches, an effect possibly attributable to the increased charge densities present around sharp surface features.

3.3. Effect of Surfactant

Surfactants are widely present in environmental and other samples. It is interesting to study their effect in ASV experiments.

The voltammetric response of cadmium on a boron-doped diamond electrode was explored with square-wave anodic stripping voltammetry. First the deposition potential was investigated in the range of −1.0 V to −2.0 V (vs. SCE) using a fixed concentration of cadmium in 0.5 M acetate buffer. An increase in the magnitude of the stripping peak was observed as the deposition potential was increased, but since the onset of gas evolution occurred at −1.9 V and beyond, the reproducibility was adversely affected. A relatively large deposition potential of −1.8 V was consequently used throughout, as it provided the clearest stripping signals possible without interference from gas evolution. Using this deposition potential, the effect of increasing cadmium concentration in 0.5 M acetate buffer was studied. Applying a 60 second deposition time at −1.8 V followed by a potential sweep, a linear response of the peak current on the cadmium concentration was observed over the range 0.2–3.0 μmol dm^{-3}. Figure 4a shows the observed voltammograms, in which the successively increasing peaks correspond to successive additions of $CdNO_3$.

The limit of detection (based on three sigma) [13] was found to be 2.5×10^{-8} mol dm^{-3}. We turn to investigating the benefits of applying an acoustic field during the deposition procedure. Using an optimized ultrasonic power of 155 W cm^{-2} and a 14 mm horn-to-electrode distance, a 60 second deposition at −1.8 V was explored with increasing concentrations of cadmium. The voltammetric response is depicted in Figure 4b, again with successively larger peaks corresponding to successive additions of $CdNO_3$. The limit

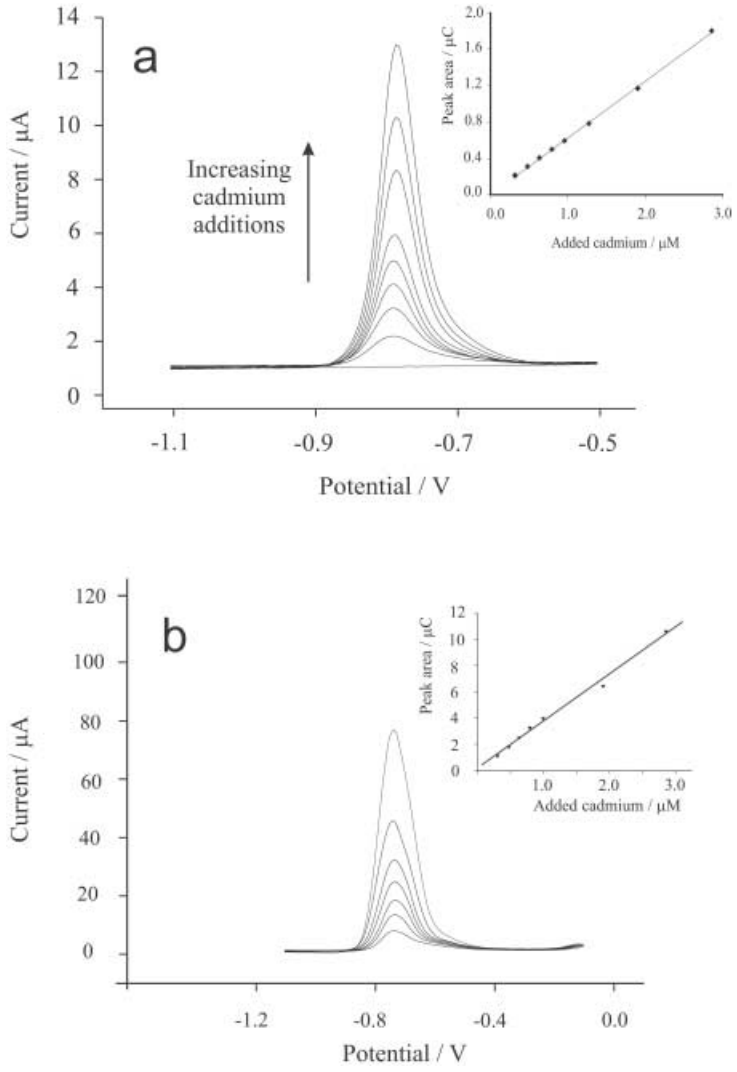

Fig. 4. SW-ASV for increasing additions of $CdNO_3$ to 0.5 M acetate buffer using a 60 s deposition at 1.8 V (vs. SCE). a) Silent conditions; successively increasing peaks correspond to cadmium concentrations of 0, 0.31, 0.48, 0.64, 0.79, 0.95, 1.27, 1.90 and 2.86 μM. b) insonated conditions (155 W cm^{-2}). Successively increasing peaks correspond to cadmium concentrations of 0.31, 0.48, 0.64, 0.79, 0.95, 1.90 and 2.86 μM. Inserts show calibration plots for the corresponding voltammograms.

of detection was found to be 4×10^{-9} mol dm^{-3}. The enhanced deposition in the presence of the acoustic streaming regime enhanced the sensitivity from 0.6 μA μM^{-1} to 3.8 μA μM^{-1} between the silent and insonated procedures.

Next, the voltammetry in the presence of a surfactant was investigated. A 60 second deposition at −1.8 V of increasing additions of cadmium to 0.5 M acetate buffer in the presence of 3 μM Triton X-100 resulted in a non-linear response of peak current versus concentration; the response was three times lower than for the quiescent surfactant free case. To attempt to alleviate this, we examined the acoustically assisted methodology in the presence of the surfactant Triton X-100. The application of 155 W cm^{-2} ultrasound during a 60 second deposition step at −1.8 V (vs. SCE) in the presence of Triton X-100 was explored. No significant current rise was observed.

Changing the ultrasonic intensity in the range 80–350 W cm^{-2} and the horn-to-electrode distance in the range 5–30 mm still did not improve the magnitude of the voltammetric response. Cadmium nucleation was confirmed by ex situ AFM analysis after deposition for 60 s from a solution of 2.1 mM cadmium in 0.5 M acetate buffer. Figure 5a shows the deposits are ca. 1 μM in diameter. Deposition in the presence of 3 μM Triton X-100 is shown in Figure 5b, where it is evident that there is little difference in the radii of the deposited cadmium nuclei. Complementary optical data from the deposition of 1 mM cadmium in 0.5 M acetate buffer in the presence and absence of the surfactant was investigated (see Figure 6). The images confirm the nucleation is progressive, while the number of nuclei in the absence of the surfactant was measured at 1.9×10^5 nuclei cm^{-2} compared to 1.1×10^4 nuclei cm^{-2} in the presence of the surfactant; the primary effect of the surfactant is to inhibit nucleation and lower growth of the metal on the electrode surface.

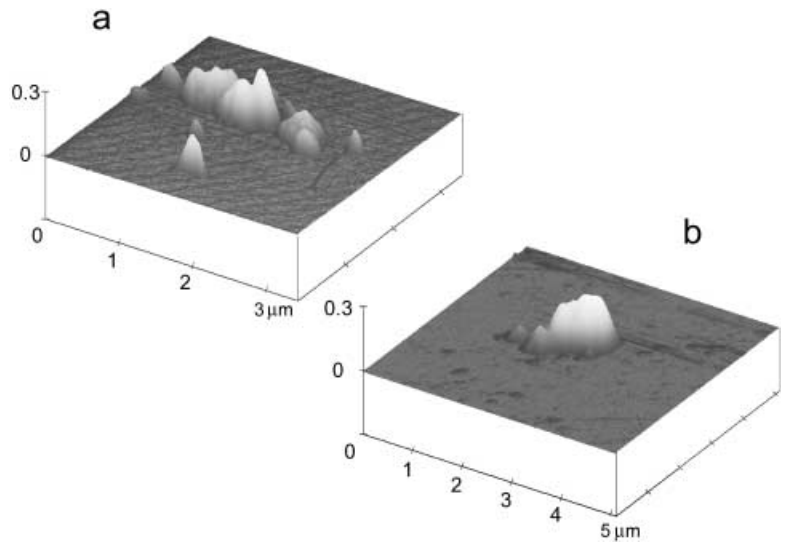

Fig. 5. AFM images after the deposition of cadmium from a solution containing 2.1 mM $CdNO_3$ in 0.5 M acetate buffer using a 60 second deposition procedure at −1.8 V (vs. SCE). a) no surfactant present, b) in the presence of a 3 μM solution of the neutral surfactant Triton X-100.

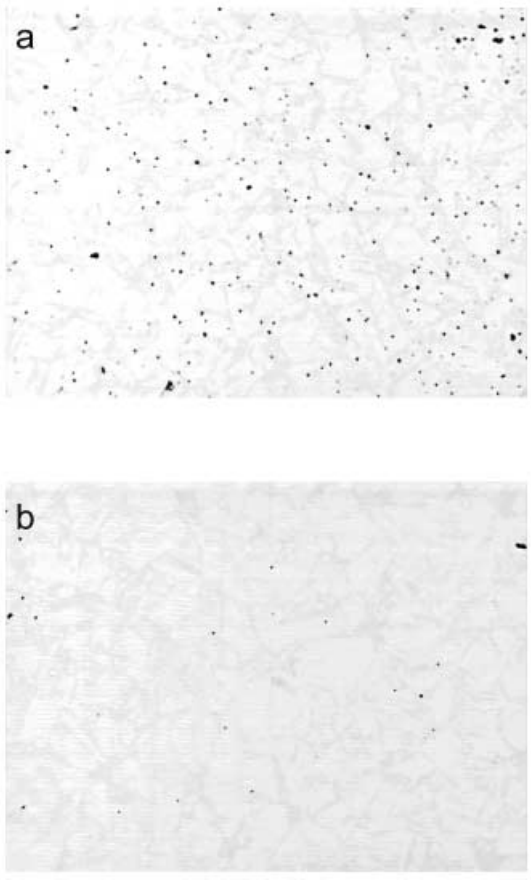

Fig. 6. Optical images of the deposition of cadmium from a solution containing 0.98 mM $CdNO_3$ in 0.5 M acetate buffer using a 60 s deposition step at −1.8 V (vs. SCE). a) no surfactant present, b) in the presence of 3 μM Triton X-100.

Chronoamperometry was used to explore the nucleation of cadmium. The current response from a solution of 2.1 mM cadmium in 0.5 M acetate buffer using an interval time of >1.5 s with a potential of −1.8 V for 60 seconds was investigated. It was observed that the chronoamperometric curve obtained in the presence of the surfactant passed less charge than that seen for the surfactant free case. We conclude that the surfactant affects the nucleation of cadmium on boron-doped diamond rather than the stripping step.

It is clear that if ASV is to be used for the successful detection of cadmium in the presence of surfactant then sample pre-treatment to destroy the inhibitor is essential.

4. Incomplete Stripping During ASV

When performing an anodic stripping voltammetry experiment, it is necessarily assumed that the stripping current is directly representative of the amount of material placed on the electrode surface during the deposition stage. However, this is not always the case.

At high solution concentrations, incomplete stripping is especially evident: Figure 7 shows successive optical images of a BDD electrode during an in situ ASV experiment using 5 mM $AgNO_3$. The first image shows a thoroughly polished electrode, upon which no deposit is visible. The second, showing considerable surface coverage, is after 180 s deposition at −0.15 V (vs. Ag.) The third, after a linear sweep from −0.15 V to +0.2 V at 20 mV s^{-1}, shows that there is still a significant amount of the material on the surface. The approximate level of surface coverage proportional to the maximum amount at ten second intervals during the deposition and stripping is shown in Figure 8,

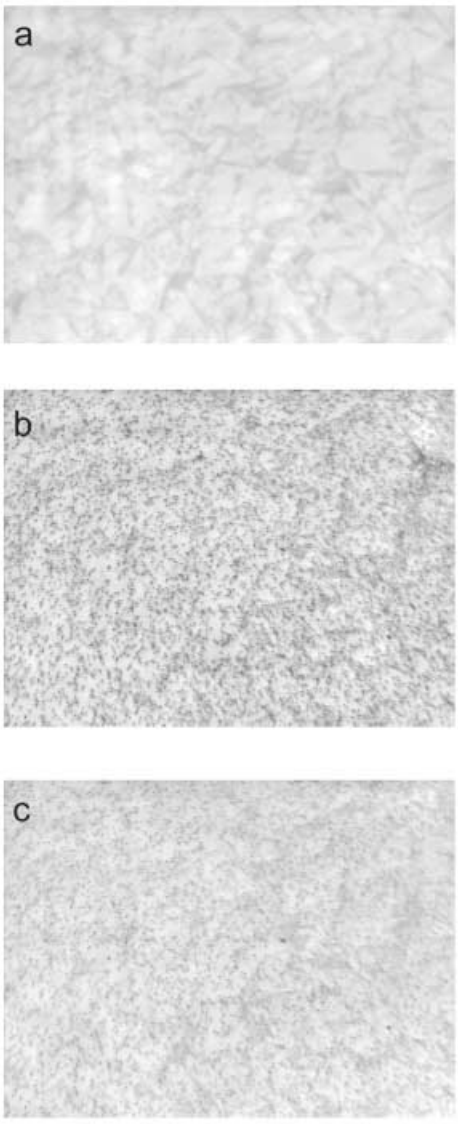

◀ Fig. 7. In situ microscopic images showing a) a clean BDD electrode, b) substantial deposition from a 5 mM $AgNO_3$/0.1 M HNO_3 solution at −0.15 V (vs. Ag) after 10 s, and c) a significant amount of material still present on the electrode surface after a linear sweep from −0.15 V to +0.2 V at 20 mV s^{-1}.

along with the potential applied; after the linear sweep is finished, roughly 60% of the deposited material remains. In fact, the remaining material could not all be removed voltammetrically, either by longer stripping times at +0.2 V or increasing the stripping potential.

The same effect may be seen when depositing lead from a 5 mM solution. Figure 9a shows an ex situ AFM image of a thoroughly clean electrode – some residue is present (probably polishing compound), but there is no other height variation of more than approximately 20 nm over the 50 μm range of the scan. After deposition at −0.55 V (vs. SCE) for 60 s, a similar area of the electrode was imaged (in order to minimize misleading results from large scale electrode inhomogeneities – see section 1). A large amount of deposit is visible (Figure 9b), while after a linear sweep from 0 V to +0.4 V (vs. SCE) at 20 mV s^{-1}, approximately 5% of the deposit (by volume) remains (Figure 9c). Again, these remaining deposits proved impossible to entirely remove voltammetrically.

To investigate ASV under conditions more similar to those in a typical ASV experiment, the above procedure was repeated with a solution containing 50 μM $AgNO_3$ and 0.1 M HNO_3. Again at each stage of the experiment, the electrode surface was imaged using ex situ AFM with a scan range of 50 μm. Figure 10 shows the results: After deposition at −0.5 V (vs. Ag)for 10 minutes, a significant amount of deposition is apparent. Stripping, as before, from −0.15 V to +0.2 V at 20 mV s^{-1} reveals that approximately 20% of the silver remains on the surface.

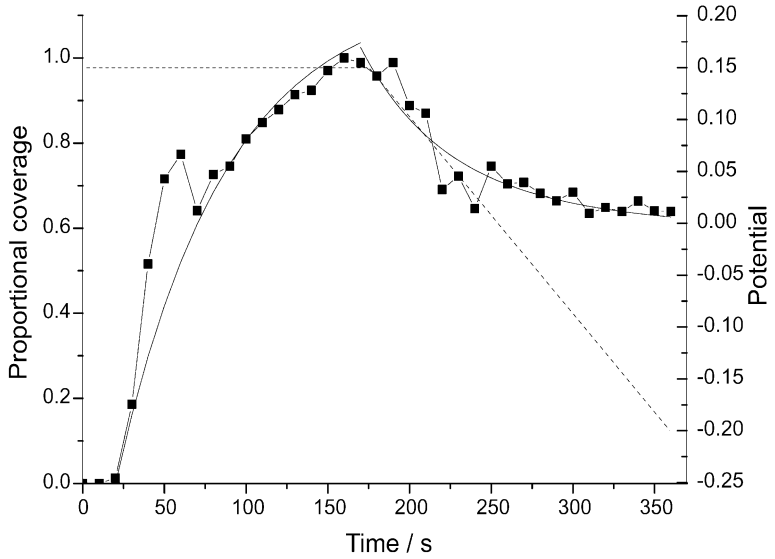

Fig. 8. Approximate relative amount of material observed on a BDD electrode during an ASV experiment in which silver was deposited from a solution containing 5 mM $AgNO_3$/0.1 M HNO_3; the applied potential vs. Ag is indicated by the dotted line (right axis). Squares show measured data, solid lines show best fits (left axis).

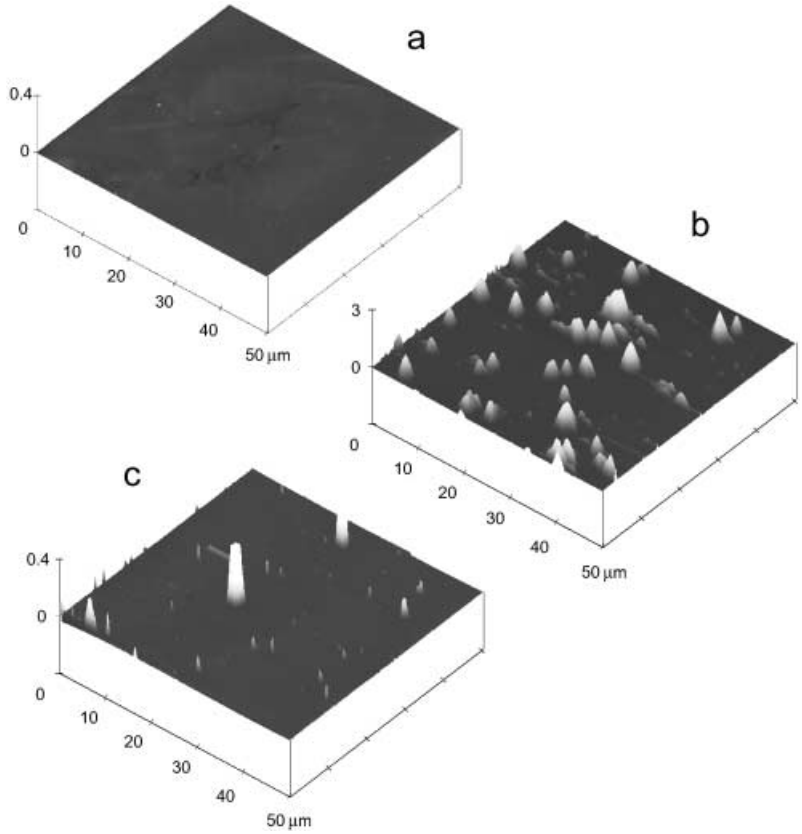

Fig. 9. Successive AFM images of a similar region of a BDD electrode. a) a thoroughly polished electrode, showing essentially no surface features. b) after deposition from a 5 mM $PbNO_3$/0.1 M HNO_3 solution at -0.55 V (vs. SCE) for 60 s. c) after a linear sweep from 0 V to $+0.4$ V (vs. SCE) at 20 mV s^{-1}.

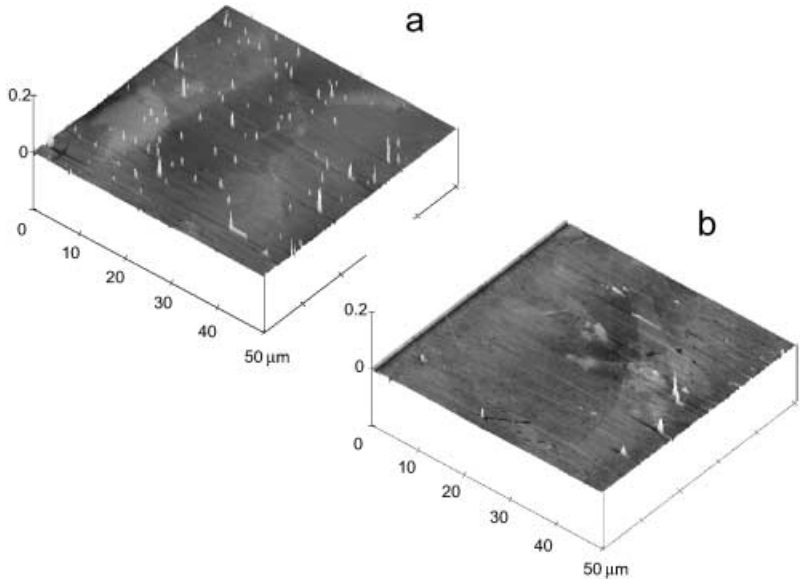

Fig. 10. Successive AFM images of a similar region of a BDD electrode. a) after deposition from a 50 μM $AgNO_3$/0.1 M HNO_3 solution at -0.5 V (vs. Ag) for 10 min. b) after a linear sweep from -0.15 V to $+0.2$ V at 20 mV s^{-1}. For an image of the electrode before deposition, see Figure 9a.

Lead ASV at low concentration shows a similar effect: deposition from a 50 μM $PbNO_3$/0.1 M HNO_3 solution at -0.8 V (vs. SCE) for 10 minutes produced a small but detectable deposit (Figure 11). After a linear sweep from 0 V to $+0.4$ V (vs. SCE) at 20 mV s^{-1}, approximately 5% of the deposit volume remains on the surface. In both the cases

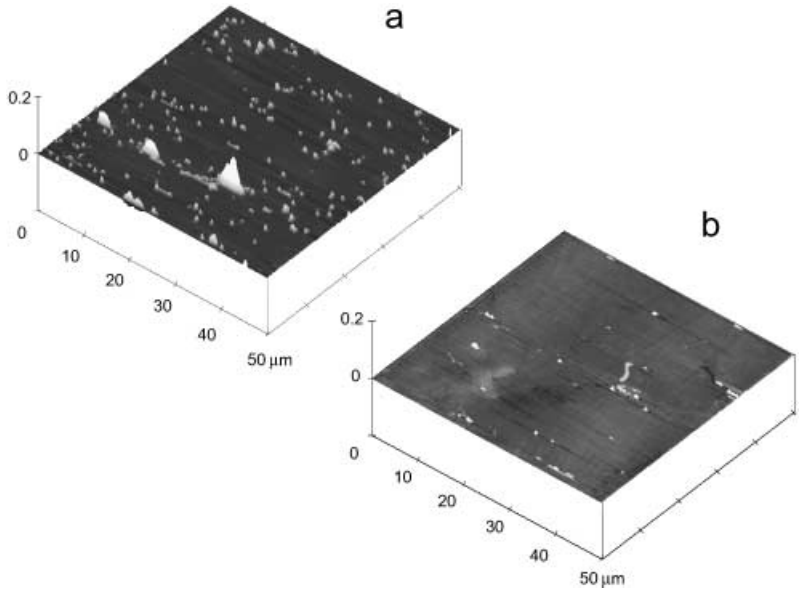

Fig. 11. Successive AFM images of a similar region of a BDD electrode. a) after deposition from a 50 μM $PbNO_3$/0.1 M HNO_3 solution at −0.8 V (vs. SCE) for 10 min. b) after a linear sweep from 0 V to +0.4 V at 20 mV s^{-1}. For an image of the electrode before deposition, see Figure 9a.

of 50 μM silver and 50 μM lead deposition, it was again found that some of the deposit could not be removed by longer stripping times or a higher stripping potential.

To further characterize the behavior of these irremovable deposits, the BDD electrode was first thoroughly cleaned using alumina polishing paste. Three successive cyclic voltammograms were then obtained, allowing a comparison between the behavior of a polished electrode and one having some residue present. The results for both 50 μM silver and lead are shown in Figure 12. It is evident that in both cases, the first scan shows a smaller deposition current and smaller stripping peak than the second and third, which are very similar to each other. Qualitatively the increase in the size of both deposition and stripping peaks is consistent with the presence of larger metal nuclei at the start of the deposition process. This is evident when we consider the diffusion-controlled current to an array of independent hemispheres: the larger initial surface area available for deposition results in a greater charge transfer and hence growth rate, and, assuming this deposition is reversible, the same applies on the stripping step.

Finally, to further study the relationship between deposition and stripping peak size, ASV experiments were performed in which chronoamperometry was used to deposit the metal, then a linear sweep to remove it. Deposition was performed for 1, 2 and 5 minutes at −0.6 V (vs. SCE) in 50 μM $PbNO_3$ and −0.8 V (vs. Ag) in 50 μM $AgNO_3$ on the BDD electrode. The linear sweep was from −0.1 V to +0.4 V (vs. Ag) in the silver solution and +0.1 V to +0.5 V in the lead solution, both at 20 mV s^{-1}. After manually cleaning the electrode, each experiment was repeated once to compare the freshly cleaned result with the electrochemically stripped result. The deposition current could not be compared directly to the stripping current due to some hydrogen evolution, particularly at the relatively high deposition overpotentials used, but it was possible to compare the size of the stripping peak as a proportion of the size of the deposition current between the first and second scan. In each experiment, it was found that the second stripping peak as a proportion of the deposition peak was consistently roughly 1.5 times larger than the first. In the context of incomplete stripping, this is consistent with less material being removed than is deposited on the first scan, while on successive scans a larger proportion (or all) of the freshly deposited material is removed, while some irremovable deposit remains.

5. Conclusions

Some of the major problems associated with quantitative anodic stripping voltammetry on inhomogeneous solid electrodes (specifically glassy carbon and boron-doped diamond films) have been illustrated. These include long range differences in the rate of material deposition, effects due to local surface features such as mechanical polishing scratches on GC and crystal faces on BDD, inhibition of deposition owing to the presence of surfactant, and incomplete removal of deposited material during the stripping step. Although only carbon electrodes were used in the described experiments, we assume that the generic problems highlighted are equally applicable to other solid stripping electrodes.

Although these observations do not necessarily preclude accurate use of ASV, it is clear that empirical ASV is a technique potentially fraught with danger. As such, we strongly recommend the use of techniques such as AFM to thoroughly characterize the electrode surface before, during

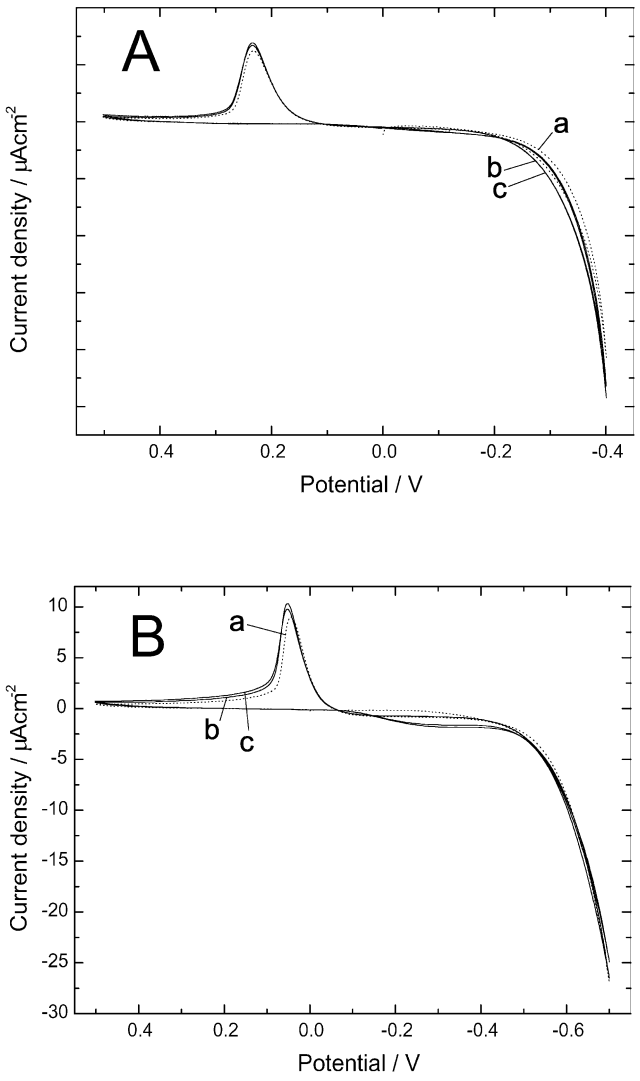

Fig. 12. Cyclic voltammograms for A) 50 μM $AgNO_3$/0.1 M HNO_3 (potentials reported vs. Ag) and B) 50 μM $PbNO_3$/0.1 M HNO_3 (potentials reported vs. SCE) on BDD. In each case the scan rate was 50 mV s^{-1} and scans a, b and c show successive scans after manually polishing the electrode.

and after the experiment, to ensure that all the processes occurring are well understood. To acquire reproducible and accurate stripping data, we have shown that it is desirable to use an electrode large enough for short range inhomogeneities to be averaged out, with as uniform a surface as possible. Precautions should be taken to eliminate (or minimize) incomplete stripping.

6. Acknowledgements

We thank the EPSRC for project studentships for MEH and CEB.

7. References

[1] K. Brainina, E. Neyman, *Electroanalytical Stripping Methods*, Wiley, New York **1993.**
[2] J. Wang, *Analytical Electrochemistry*, Wiley-VCH, New York, N. Y. **2000.**
[3] A. Bond, *Bondening Electrochemical Horizons*, Oxford University Press **2002.**
[4] J. Wang, J. Lu, S. B. Hocevar, P. A. M. Farias, B. Ogorevc, *Anal. Chem.* **2000**, *72*, 3218.
[5] C. Agra-Gutiérrez, J. L. Hardcastle, J. C. Ball, R. G. Compton, *Analyst* **1999**, *124*, 1053.
[6] http://www.planetark.org/dailynewsstory.cfm?newsid = 2382&newsdate = 06-Nov**1998.**
[7] E. Gustafsson., *Water Air and Soil Pollution*, **1995**, *80*, 99.
[8] J. Wang, J. Lu, *Electrochem. Commun.* **2000**, *2*, 390.
[9] M. E. Hyde, R. Jacobs, R. G. Compton, *J. Phys. Chem. B* **2002**, *106*, 11075.
[10] M. A. Margulis, A. N. Mal'tsev, *Russ. J. Phys. Chem.* **1969**, *43*, 592.
[11] R. F. Contamine, A. M. Wilhelm, J. Berlan, H. Delmas, *Ultrason. Sonochem.* **1993**, *2*, S43.
[12] C. E. Banks, R. G. Compton, *Electroanalysis* **2003**, *15*, 329.
[13] C. Brett, A. M. O. Brett, *Electroanalysis*, Oxford University Press, Oxford, UK **1998.**